Fe-N-Carbon aerogel catalyst for oxygen reduction reaction

Hongxin Ge, Frederic Jaouen, Nicolas Bibent, Kavita Kumar, Laetitia Dubau, Frédéric Maillard, Sandrine Berthon-Fabry

Fe-N-Carbon aerogel catalyst for oxygen reduction reaction

Hongxin Ge (1), Frédéric Jaouen (2), Nicolas Bibent (2), Kavita Kumar (3), Laetitia Dubau (3), Frédéric Maillard (3), Sandrine Berthon-Fabry (1)

(1) *MINES ParisTech, PSL University PERSEE - Centre procédés, énergies renouvelables et systèmes énergétiques, CS 10207 rue Claude Daunesse F-06904 Sophia Antipolis Cedex, France*.

(2) *ICGM - UMR 5253, 2 Place Eugène Bataillon, 34090 Montpellier, Montpellier, France*

(3) *Univ. Grenoble Alpes, Univ. Savoie Mont Blanc, CNRS, Grenoble INP, LEPMI, 38000 Grenoble, France*

Tel.: +33 493957547

Fax: +33 493957535

sandrine.berthon-fabry@mines-paristech.fr

Abstract

Proton exchange membrane fuel cell (PEMFC)s are an excellent energy conversion device for wide application of hydrogen, especially for portable or transportation applications. To reduce the total cost of these devices, non-precious-metal catalysts (NPMCs) have shown promises in replacing platinum-based catalysts. Among NPMCs, iron-nitrogen-carbon (Fe-N-C) catalysts subclass are the most mature. These catalysts are based on nitrogen (N) coordinated iron (Fe) ions embedded in a carbon (C) matrix acting as catalytically active centers. Numerous studies have focused on promoting their catalytic performance towards the oxygen reduction reaction (ORR). Nevertheless, such materials remain less performant than carbon-supported platinum nanoparticles (Pt/C), leading to *ca.* 3-10 times thicker cathodes, and associated mass transport limitations.

Carbon aerogels are ideal candidates to synthesize Fe-N-C catalysts with tuneable mass transport properties thanks to their tridimensional open texture, tailored pore size distribution from micro to macropores and their good electrical conductivity. Herein, we show the promises of Fe-N-C aerogels synthesized a “one pot” sol-gel method comprising formation of a Fe-doped resorcinol (R)-formaldehyde (F)-melamine (M) hydrogel, and followed by carbon dioxide (CO_2) supercritical drying, and high temperature pyrolysis under N_2 and NH_3 atmosphere. By introducing ligands in the synthesis mixture, we modified the chemical environment of the Fe precursor. The resulting changes in morphology, ORR activity and mass transport properties are investigated a rotating disk electrode (RDE) set-up and a PEMFC device.

Introduction

Proton exchange membrane fuel cell (PEMFC) is a promising device for wide application of hydrogen, especially for portable and transportation applications. In a PEMFC, hydrogen is oxidized at the anode, and oxygen is reduced into water at the cathode. Due to sluggish oxygen reduction reaction (ORR) kinetics, large quantity of catalyst is necessary at the cathode to enhance the efficiency of the device. Currently, carbon-supported platinum (Pt)-based nanoparticles is the most state of art catalyst, but Pt is an expensive and rare element, which constrains the commercialization of PEMFCs. To reduce the cost of these devices, the demand of developing alternative non-precious-metal catalysts (NPMCs) becomes urgent, and investigations to replace Pt-based catalysts are carried out. Among them, iron-nitrogen-carbon (Fe-N-C) catalysts subclass is the most promising.

1. Scientific Approach

Numerous studies have focused on promoting the catalytic performance and exploring the ORR mechanism of Fe-N-C catalysts. [1]–[4] These are usually synthesized through pyrolysis of Fe, N and C precursors at high temperature. Such high-temperature treatment leads to a wide variety of moieties, which can be divided in two main categories: (i) the Fe-free moieties and (ii) the Fe-containing moieties. [5]–[7] Using extended X-ray absorption fine structure and ^{57}Fe Mössbauer spectroscopy, Zitolo *et al*. revealed that the enhancement of the ORR activity is directly related to the existence of porphyrin-like FeN_4C_{12} moieties. [8] Many attempts have been made to increase the density of these active sites. Pyrolysis under NH_3 revealed best adapted, because NH_3 etches the most disordered regions of the carbon matrix during pyrolysis, leading to the formation of micropores-hosted Fe-N_x sites. [9] Fe-N-C catalysts with enhanced ORR activities were also prepared by using precursors with pre-existing Fe-N coordination (Fe-phthalocyanine or Fe-phenanthroline complexes), instead of separate Fe and N precursors. [2] Despite these efforts, Fe-N-C catalysts remain still less efficient than Pt/C, and the activity difference must be offset with *ca*. 3-10 times thicker PEMFC cathodes. [10] Also, mass transport limitations become a concern in PEMFC devices, and need to be optimized. Large mesopore and macropore volumes are required to ensure optimal Fickian diffusion of O_2 and ORR product (H_2O). [11] The ideal texture of Fe-N-C materials should thus combine micropores (hosting the active sites) and mesopores/macropores (allowing Fickian diffusion of O_2 and H_2O).

Due to their high specific surface area and tuneable pore size distribution (at micro, meso and macro scales), carbon aerogels are ideal candidates to synthesize highly performant Fe-N-C catalysts. Carbon aerogels are commonly prepared by pyrolysing an organic aerogel of resorcinol (R) and formaldehyde (F).[12]–[15] As for traditional Fe-N-C catalysts, N can be introduced by adding melamine (M) during the polymerization process.[16]–[18] The Fe, N-doped carbon aerogel is promising to present both high ORR activity and mass transport properties. Nagy *et al*. demonstrated that N-doped carbon aerogels without metal could perform high specific surface area,[16],[19] and our previous research found that iron doping could greatly enhance the ORR activity of aerogel. [20] Herein, we synthesized Fe-N-C aerogel catalysts using a “one pot” sol-gel method comprising formation of a Fe-doped resorcinol (R)-formaldehyde (F)-melamine (M) hydrogel, and followed by CO_2 supercritical drying and pyrolysis under N_2 and NH_3 atmosphere. By adding ligands, namely ethylenediaminetetraacetic acid (EDTA) or 1,10-phenanthroline (Phen), we modified the chemical environment of the Fe precursor. The resulting changes on the physicochemical characteristics were investigated using scanning electron microscopy (SEM), nitrogen

sorption isotherms, X-ray photoelectron spectroscopy (XPS), inductively coupled plasma mass spectrometry (ICP-MS) and X-ray diffraction (XRD) analysis. The performance of the synthesized Fe-N-C materials was then evaluated using rotating disk electrode (RDE) set-up and membrane-electrode-assemblies (MEAs).

2. Experiments

Sample synthesis

The Fe-N-C catalysts were prepared inspired from the method described by us before, and resorcinol (R), formaldehyde (F), melamine (M), and $(NH_4)_2Fe(SO_4)_2$ as precursors.[20] Sodium carbonate (NaC) was used to promote the polymerization in deionized water (W). Two different ligands (EDTA and Phen) were introduced in the synthesis solution to investigate if Fe-coordination could enhance the ORR activity of the synthesized catalysts. The reactants and solvent were mixed at 70 °C with the molar ratio of 2:7:1:0.033:60: for R:F:M:NaC:W. $(NH_4)_2Fe(SO_4)_2$ was added with a stoichiometry R:Fe of 1:0.015, targeting *ca*. 1 wt. % Fe in the final catalysts. For ligand-containing catalysts, the EDTA or Phen was firstly mixed with the Fe precursor in deionized water to form the complex with molar ratio of 1:1 or 1:3, respectively and then added into the mixture solution. Subsequently, the pH of solution was adjusted to 8 by adding NaOH solution under continuous stirring until the gel formed. The hydrogel was then aged in a water bath at 70 °C for 120 h. The obtained hydrogels were subjected to a water-acetone exchange and then to CO_2 supercritical drying. Subsequently, the aerogels were pyrolysed at 800 °C under N_2 flow for 1 h, smashed by ball-milling method and washed with 0.5 M H_2SO_4 to remove Fe nanoparticles, which were possibly generated during the pyrolysis. In order to increase the density of active sites, a second heat treatment was conducted at 950 °C under NH_3 atmosphere.

Physicochemical characterization

The Fe content in the catalysts was determined by ICP-MS. XRD analysis was performed using an X"pert Pro Philips diffractometer using filtered Cu *K*α radiation (λ=0.15418 nm) generated at 40 kV and 30 mA. The morphologies of the catalysts were determined by SEM (ZEISS SUPRA^{TM}40) operated at 3.0 kV. The detailed specific surface areas were measured by nitrogen sorption isotherms at 77 K with a Micromeritics ASAP 2020 instrument, and the pore size distribution was calculated using the 2D-NLDFT-Heterogenerous Surface method based on the adsorption isotherms. XPS was used to identify the elemental composition of the surface of the catalysts. The measurements were performed using Thermo Scientific^{TM} K-Alpha^{TM} spectrometer equipped with an Al *K*α1,2 monochromatic source (1486.6 eV).

Electrochemical measurements

Rotating disk electrode (RDE) measurements were performed under atmospheric pressure and room temperature in a three-electrode cell. The reference electrode was a reversible hydrogen electrode (RHE) and the counter electrode was a graphite electrode. The catalyst ink was prepared by ultra-sonicating 10 mg catalyst powder, 95 µL 5 wt. % Nafion, 752 µL ethanol, and 46 µL deionized water for 1 h. 7 µL of this ink was dropped on a 0.196 cm^2 glassy carbon disk, resulting in a catalyst loading of 0.4 $mg_{Fe\text{-}N\text{-}C}/cm^2$. The ORR activities were measured in O_2-saturated 0.05 M H_2SO_4 aqueous solution. Linear scan voltammograms were recorded (LSV) at 10 mV/s from 1.1 to 0 V *vs*. RHE under constant revolution rate (1600 rpm). The same test was repeated in N_2-saturated electrolyte to eliminate the pseudo-capacitive current ('background' current). Cyclic voltammograms between 0 and 1.0 V vs. RHE were measured at 10 mV/s in N_2-saturated electrolyte.
For PEMFC testing, 20 mg of catalyst, 915 µL 5 wt. % Nafion solution, 63 µL of 1-propanol, and 272 µL of deionized water were mixed and subjected to sonication for 1 hour. The ink

was deposited on a 4.84 cm^2 gas diffusion layer as the cathode, resulting in a catalyst loading of 4.1 $mg_{Fe\text{-}N\text{-}C}/cm^2$. The cathode was then dried at 80 °C, and hot-pressed at 135 °C with a Pt/C anode and a Nafion membrane. The temperature of cell was stabilized at 80 °C during the test and the relative pressure of H_2 and O_2 was 1 bar.

3. Results

The synthesized catalysts are listed in Table 1, along with the results of their physicochemical and electrochemical characterizations. $(NH_4)_2Fe(SO_4)_2$ was selected as Fe precursor because of the high solubility of Fe^{2+} compared to Fe^{3+} in aqueous solution of pH 8 (solubility product constant (K_{sp}) of 2.79×10^{-39} and 4.87×10^{-17} for $Fe(OH)_3$ and $Fe(OH)_2$, respectively). [21] The ligands (EDTA or Phen) were introduced to modify the solubility of Fe ions in the precursor solution (resulting to a different dispersion of Fe atom in the carbon aerogel) and coordinate Fe^{2+} to form preexisting Fe-N bonds, leading to better ORR activity.[2]

Table 1. Physicochemical and electrochemical characterization of catalysts prepared with different ligands.

Iron precursor	Ligand	ICP		BET surface (m^2/g)	V_{total} (cm^3/g)	V_{micro} (cm^3/g)	V_{meso} (cm^3/g)	Current density ($A/g_{Fe\text{-}N\text{-}C}$)			XPS			
		Fe wt. %	Fe at. %					RDE at E = 0.8 V *vs.* RHE	PEMFC at U = 0.8 V	PEMFC at U = 0.5 V	C at. %	N at. %	O at. %	Fe at. %
$(NH_4)_2Fe(SO_4)_2$	EDTA	0.16	0.03	1274	1.63	0.37	1.21	1.01	2.00	89.7	93.92	3.30	2.72	0.06
	Phen	0.73	0.16	1455	2.32	0.43	1.83	1.74	1.21	74.7	93.20	2.76	3.85	0.20
	-	0.70	0.15	1665	1.92	0.46	1.34	1.89	9.44	150.1	95.37	3.08	1.38	0.18

The Fe content in the final catalyst was determined using ICP-MS and XPS, and the results are listed in **Table 1**. Similar values obtained from the two methods suggesting a uniform distribution of Fe atoms both in the bulk and at the surface. The Fe content was close to the targeted value (1 wt. %) for the catalysts synthesized using exclusively the Fe precursor or the Fe precursor + Phen, but it revealed extremely low for the catalyst prepared using Fe + EDTA. We relate this result to the enhanced solubility of Fe ions resulting from EDTA addition. Indeed, during the solvent exchange (between water and acetone for CO_2 supercritical drying), the solvent became slightly coloured, suggesting that the complex was more soluble in water than in acetone, and accounting for the Fe content loss.

Morphology and porosity of catalysts

The SEM images displayed in Figure 1 (a)-(c) provide insights into the porosity of the synthesized catalysts. Similar texture was observed for the ligand-free and EDTA-containing catalysts. A more heterogeneous texture was observed for the catalyst prepared with Phen, probably resulting from the agglomeration of large clusters. The XRD patterns shown in Figure 1 (d) indicate that all catalysts were poorly crystallized (confirmed by Raman spectrometry). Three small peaks at 2θ = 26.4°, 34.6°, and 52.4° can be found in the pattern of Fe-Phen catalyst, but could not be attributed to any Fe-containing species (α-Fe, γ-Fe, Fe_3C or oxides). TEM images (not shown here) also confirmed that no Fe-based nanoparticles were detected in the three catalysts.

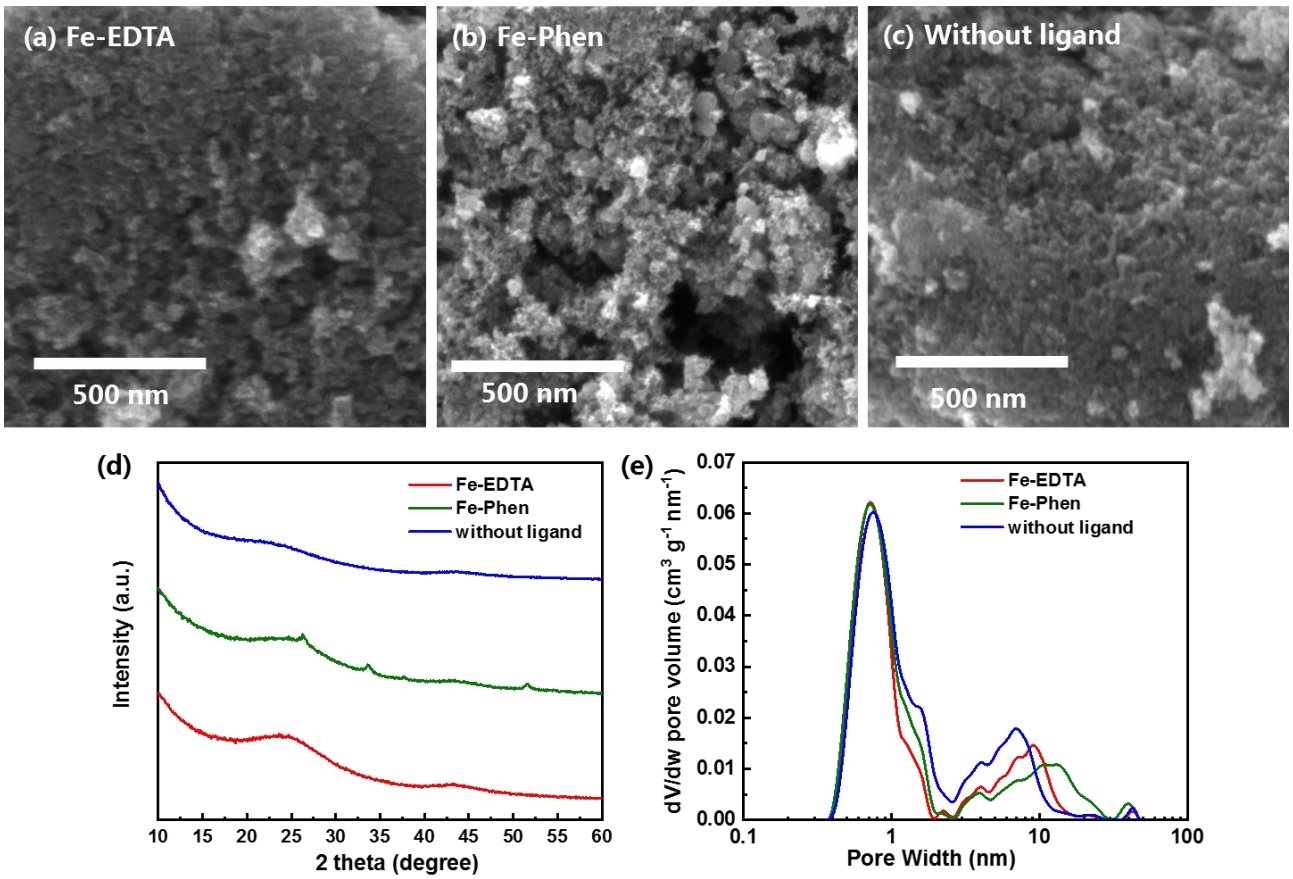

Figure 1. (a)-(c) SEM images, (d) XRD patterns and (e) pore size distribution plots derived from N_2 adsorption isotherms at 77 K for the synthesized catalysts.

Figure 1 (e) shows the pore size distribution of catalysts derived from N_2 adsorption isotherms at 77 K, and the microporous and mesoporous volumes of the catalysts are listed in Table 1. In agreement with SEM images, the ligand-free and Fe-EDTA catalysts exhibit similar mesopore distribution (centered around 6-10 nm), suggesting that EDTA mildly affected the poly-condensation process. In contrast, the catalyst prepared with Phen featured larger mesopores size distribution with size centered around 20 nm: this may result from a different poly-condensation mechanism caused by the presence of Phen. Similar micropore size distributions were observed for the three catalysts. Such result makes sense if one considers that micropores are mainly generated during the thermal treatment (pyrolysis under N_2 and then NH_3) process,[9],[20] and that identical conditions were used for all catalysts.

Electrochemical characterization

The impact of ligand additives on the ORR activity of the Fe-N-C catalysts were firstly evaluated using rotating disk electrode set-up. The polarization curves of catalysts are shown in Figure 2 (a) and the kinetic currents at E = 0.8 V *vs*. RHE (corrected from Ohmic drop, pseudocapacitive current and from O_2 transport in solution) are listed in Table 1. Clearly, the ligand-free Fe-N-C catalysts was the more active, with a current density of 1.89 $A/g_{Fe\text{-}N\text{-}C}$ at E = 0.8 V vs RHE. Due to similar Fe content the Fe-Phen featured similar mass-normalized ORR activity. The poor ORR activity of catalyst Fe-EDTA was attributed to its low Fe content.

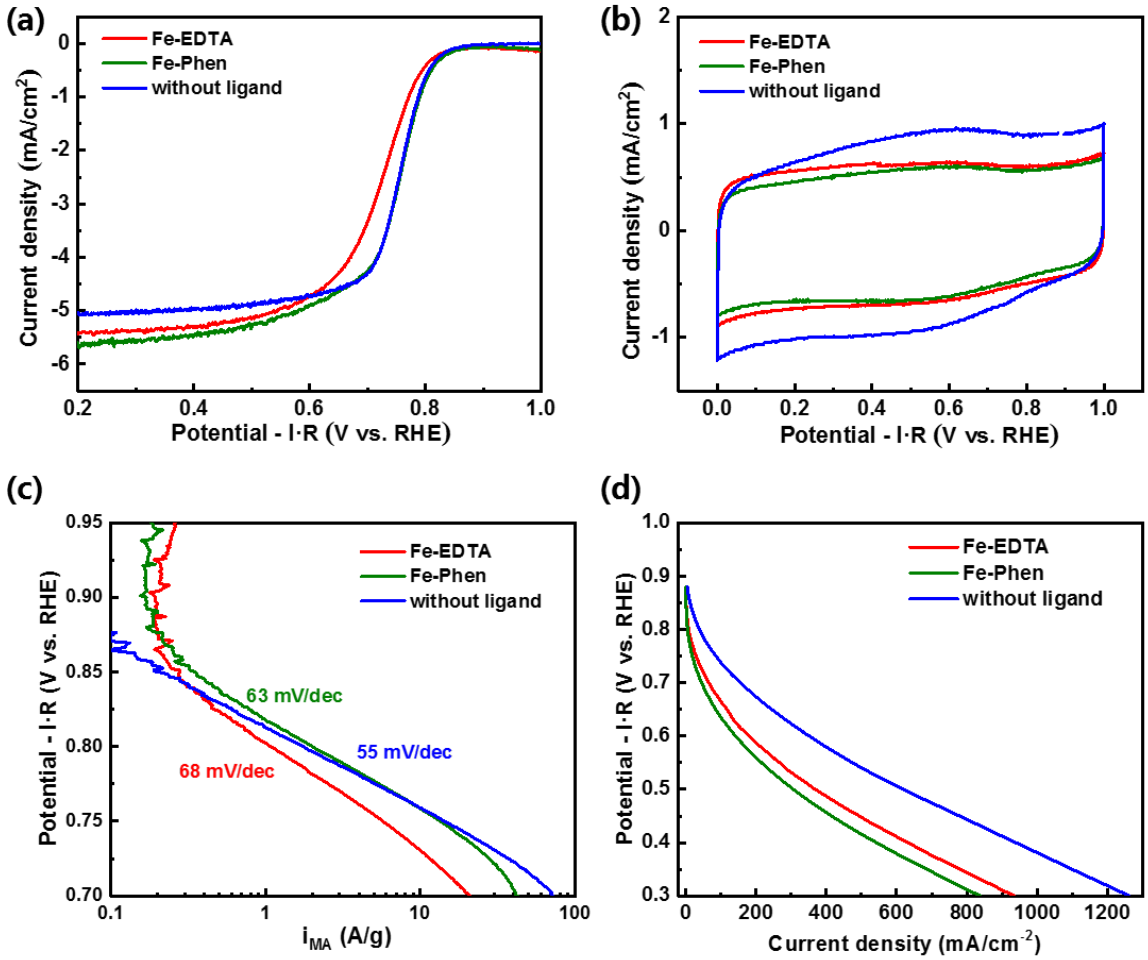

Figure 2. (a) Oxygen reduction reaction polarization curves and (b) cyclic voltammograms recorded in O_2- or N_2-saturated 0.05 M H_2SO_4 at 10 mV/s on RDE, respectively; (c) Tafel plots of the O_2-transport and background-current corrected kinetic current obtained from the steady-state *I–E* curves at ω= 1600 rpm, and (d) iR-free polarization curves recorded in PEMFC devices for the catalysts synthesized in this work (*T* = 80°C, 100 % RH, PO_2 = 1 bar, 150 mL/min).

The Tafel slopes, calculated from O_2-transport and background-current corrected polarization curves, shown in Figure 2 (c), were close to 60 mV/dec for all catalysts. Although different from the predicted value of 120 mV/dec assuming a one-electron transfer in the rate-determining step and a symmetry factor of 0.5, similar Tafel slopes indicate that the ORR mechanism remains identical on the different catalysts. Similar Tafel slopes but different ORR mass activities at *E* = 0.80 V *vs*. RHE also suggest that different mass-normalized densities of active sites or different turnover frequencies (number of electrons transferred per site per second) for the synthesized catalysts. [22] These were then implemented in membrane-electrode assemblies (MEA), and tested in PEMFC configuration. The current densities measured at *E* = 0.8 V *vs.* RHE (RDE configuration) or at *U* = 0.8 V (MEA configuration) are listed in Table 1. Better PEMFC performance was observed for the catalysts featuring the larger electrochemical available area according to the CV curves shown in Figure 2(b). A 5-fold enhancement of the catalytic performance was monitored for the ligand-free Fe-N-C catalyst, but the enhancement was only 2-fold and < 1 for the Fe-EDTA and Fe-Phen catalysts, respectively. Besides, these enhancement factors are far from that calculated (26-fold) using Arrhenius law and the activation energy of 61.8

kJ/mol determined at zero overpotential from MEA data by Osmieri *et al.*[23] These results clearly suggest that, besides pure charge-transfer limitations, other characteristics, such as the accessibility of O_2 and H^+ to the active sites limit the performance in PEMFC configuration. It is important that the polarization curves do not collapse at high current densities (j > 0.5 A/cm$^2_{geo}$), demonstrating the excellent mass transport properties of carbon aerogels.

Conclusion

Fe-N-C aerogel catalysts with high porosity and good ORR activity were synthesized using a one-pot sol gel method, based on the polymerization of resorcinol, melamine and formaldehyde in the presence of $(NH_4)_2Fe(SO_4)_2$. Two ligands (EDTA or 1,10-phenanthroline) were integrated in the synthesis, and their impact on pore size distribution and ORR activity was investigated. The Fe-EDTA catalyst exhibits similar pore size distribution with the ligand-free Fe-N-C catalyst; however the enhanced solubility of Fe(II)-EDTA complex leads to loss of Fe during the solvent exchange step, and reduces the Fe content and consequently the final ORR activity. The introduction of Phen allows reaching the targeted Fe content due to a stronger interaction between Phen and the organic matrix and larger mesopore size distribution. Its ORR mass activity can also be comparable with the ligand-free Fe-N-C catalysts in RDE set-up. Polarization curves in real PEMFC device were also measured to compare with RDE results. The curves do not collapse at high current densities (j > 0.5 A/cm$^2_{geo}$) demonstrating the excellent mass transport properties of the Fe-N-C aerogels. They also present the same trends with electrochemical available areas obtained from CV curves in RDE set-up, showing that the ligand-free catalyst outperforms Fe-EDTA and Fe-Phen.

Acknowledgements

This work was supported by the French National Research Agency in the frame of the ANIMA project (grant number n°ANR-19-CE05-0039).

References

[1] Tian, J. *et al.* Optimized synthesis of Fe/N/C cathode catalysts for PEM fuel cells: a matter of iron-ligand coordination strength. *Angew. Chem. Int. Ed.* **52** (2013), 6867–6870.

[2] Li, J. *et al.* The challenge of achieving a high density of Fe-based active sites in a highly graphitic carbon matrix. *Catalysts* **9** (2019), 144.

[3] Lefèvre, M., Proietti, E., Jaouen, F. & Dodelet, J.-P. Iron-based catalysts with improved oxygen reduction activity in polymer electrolyte fuel cells. *Science* **324** (2009), 71–74.

[4] Jaouen, F. & Dodelet, J.-P. Average turn-over frequency of O2 electro-reduction for Fe/N/C and Co/N/C catalysts in PEFCs. *Electrochimica Acta* **52** (2007), 5975–5984.

[5] Guo, D. *et al.* Active sites of nitrogen-doped carbon materials for oxygen reduction reaction clarified using model catalysts. *Science* **351** (2016), 361–365.

[6] Kramm, U. I. *et al.* Structure of the catalytic sites in Fe/N/C-catalysts for O2-reduction in PEM fuel cells. *Phys. Chem. Chem. Phys.* **14** (2012), 11673.

[7] Yang, L. *et al.* Carbon-based metal-free ORR electrocatalysts for fuel cells: past, present, and future. *Adv. Mater.* **31** (2019), 1804799.

[8] Zitolo, A. *et al.* Identification of catalytic sites in cobalt-nitrogen-carbon materials for the oxygen reduction reaction. *Nat Commun* **8** (2017), 957.

[9] Jaouen, F., Lefèvre, M., Dodelet, J.-P. & Cai, M. Heat-treated Fe/N/C catalysts for O_2 electroreduction: are active sites hosted in micropores? *J. Phys. Chem. B* **110** (2006), 5553–5558.

[10] Jaouen, F. *et al.* Oxygen reduction activities compared in rotating-disk electrode and proton exchange membrane fuel cells for highly active FeNC catalysts. *Electrochimica Acta* **87** (2013), 619–628.
[11] Proietti, E. *et al.* Iron-based cathode catalyst with enhanced power density in polymer electrolyte membrane fuel cells. *Nat Commun* **2** (2011), 416.
[12] ElKhatat, A. M. & Al-Muhtaseb, S. A. Advances in tailoring resorcinol-formaldehyde organic and carbon gels. *Adv. Mater.* **23** (2011), 2887–2903.
[13] Horikawa, T., Hayashi, J. & Muroyama, K. Controllability of pore characteristics of resorcinol–formaldehyde carbon aerogel. *Carbon* **42** (2004), 1625–1633.
[14] Zhou, H. *et al.* Facile preparation and ultra-microporous structure of melamine–resorcinol–formaldehyde polymeric microspheres. *Chem. Commun.* **49** (2013), 3763.
[15] Al-Muhtaseb, S. A. & Ritter, J. A. Preparation and properties of resorcinol-formaldehyde organic and carbon gels. *Adv. Mater.* **15** (2003), 101–114.
[16] Nagy, B., Villar-Rodil, S., Tascón, J. M. D., Bakos, I. & László, K. Nitrogen doped mesoporous carbon aerogels and implications for electrocatalytic oxygen reduction reactions. *Microporous and Mesoporous Materials* **230** (2016), 135–144.
[17] Rasines, G. *et al.* N-doped monolithic carbon aerogel electrodes with optimized features for the electrosorption of ions. *Carbon* **83** (2015), 262–274.
[18] Brun, N., Wohlgemuth, S. A., Osiceanu, P. & Titirici, M. M. Original design of nitrogen-doped carbon aerogels from sustainable precursors: application as metal-free oxygen reduction catalysts. *Green Chem.* **15** (2013), 2514.
[19] Nagy, B. *et al.* Synergism of nitrogen and reduced graphene in the electrocatalytic behavior of resorcinol - Formaldehyde based carbon aerogels. *Carbon* **139** (2018), 872–879.
[20] Wang, Y. & Berthon-Fabry, S. One-pot synthesis of Fe-N-containing carbon aerogel for oxygen reduction reaction. *Electrocatalysis* **12** (2021), 78–90.
[21] R. Lide, D. *Handbook of Chemistry and Physics*. (CRC Press, 2003).
[22] Sgarbi, R. *et al.* Oxygen reduction reaction mechanism and kinetics on M-NxCy and M@N-C active sites present in model M-N-C catalysts under alkaline and acidic conditions. *J Solid State Electrochem* **25** (2021), 45–56.
[23] Osmieri, L. *et al.* Elucidation of Fe-N-C electrocatalyst active site functionality via in-situ X-ray absorption and operando determination of oxygen reduction reaction kinetics in a PEFC. *Applied Catalysis B: Environmental* **257** (2019), 117929.

Keywords: Fe-N-C catalyst, Carbon aerogels, Proton-exchange membrane fuel cell , Oxygen reduction reaction.